NAMT
93-016

Phase Field Computations of Single-Needle Crystals, Crystal Growth and Motion by Mean Curvature

G. Caginalp
University of Pittsburgh
E. Socolovsky
Hampton University

Research Report No. 93-NA-016

April 1993

Sponsors

U.S. Army Research Office
Research Triangle Park
NC 27709

National Science Foundation
1800 G Street, N.W.
Washington, DC 20550

TO APPEAR IN SIAM Journal on Scientific and Statistical Computing

PHASE FIELD COMPUTATIONS OF SINGLE-NEEDLE CRYSTALS, CRYSTAL GROWTH AND MOTION BY MEAN CURVATURE

G. CAGINALP[+] AND E. SOCOLOVSKY[*]

[+]Mathematics and Statistics Department, University of Pittsburgh
Pittsburgh, PA 15260
[*]Center for Nonlinear Analysis
Mathematics Department, Hampton University
Hampton, VA 23668

ABSTRACT. The phase field model for free boundaries consists of a system of parabolic differential equations in which the variables represent a phase (or "order") parameter and temperature respectively. The parameters in the equations are related directly to the physical observables including the interfacial width ϵ which we can regard as a free parameter in computation. The phase field equations can be used to compute a wide range of sharp interface problems including the classical Stefan model, its modification to incorporate surface-tension and/or surface kinetic terms, the Cahn-Allen motion by mean curvature, the Hele-Shaw model, etc. Also included is anisotropy in the equilibrium and dynamical forms generally considered by materials scientists. By adjusting the parameters, the computations can be varied continuously from single needle dendritic to faceted crystals.

The computational method consists of smoothing a sharp interface problem within the scaling of distinguished limits of the phase field equations which preserve the physically important parameters. The two-dimensional calculations indicate that this efficient method for treating these stiff problems results in very accurate interface determination without interface tracking. We test these methods against exact and analytical results available in planar waves, faceted growth and motion by mean curvature up to extinction time.

The results obtained for the single needle crystal show a constant velocity growth as expected from laboratory experiments.

[+]Supported by NSF Grant DMS-9002242 .

1. Introduction.

The problem of numerical computation of a moving boundary has been under active study from a number of perspectives (see [Gl] for a survey). The phase field approach to free boundaries has two salient features: (i) a broad spectrum of distinct problems can be studied by means of a single set of equations, and (ii) the interface in these problems does not need to be tracked explicitly, as the computations use a system of parabolic equations in which the interface has been diffused.

The phase field equations specifically identify all macroscopic parameters, e.g. latent heat, diffusivity, etc. and a parameter ϵ which is a measure of interface thickness.

We begin by defining a set of sharp interface problems in a spatial region $\Omega \subset \mathbb{R}^n$ with the interface defined as $\Gamma(t)$ with $t \in \mathbb{R}^+$. A basic problem is to find a temperature function $T(x,t)$ and a curve (or surface) $\Gamma(t) \subset \Omega$ which satisfy the equations.

$$\rho c_{spm} T_t = K \Delta T \qquad \text{in } \Omega \setminus \Gamma(t) \tag{1.1}$$

$$\rho l v = K \nabla T \cdot n]_+^- \qquad \text{on } \Gamma(t) \tag{1.2}$$

$$T - T_E = -\frac{\sigma}{[s]_E}\kappa - \alpha \frac{\sigma v}{[s]_E} \qquad \text{on } \Gamma(t) \tag{1.3}$$

$T_E :=$ equilibrium melting temperature

$\ell :=$ latent heat per unit mass

$K :=$ thermal conductivity

$\sigma :=$ surface tension between two phases

$\rho :=$ density

$c_{spm} :=$ specific heat per unit mass

$[s]_E :=$ entropy difference between phases per unit volume

$v :=$ normal velocity (positive if motion is directed toward liquid)

$\kappa :=$ sum of principal curvatures at the particular point on the interface

$\nabla T \cdot n]_+^- :=$ jump in the normal component of the temperature (from solid to liquid)

$\alpha :=$ kinetic undercooling coefficient

By defining a dimensionless temperature, $u := (T - T_E)c_{spm}/\ell$, a diffusion parameter $D := K/\rho c_{spm}$ and a "capillary length" $d_0 := \sigma c_{spm}/([s]_E \ell)$ one can rewrite (1.1) - (1.3) as

$$u_t = D\Delta u \text{ in } \Omega \setminus \Gamma(t) \tag{1.1'}$$

$$v = D\nabla u \cdot n]_+^- \text{ on } \Gamma(t) \tag{1.2'}$$

$$u = -d_0\kappa - \alpha d_0 v \text{ on } \Gamma(t). \tag{1.3'}$$

Note that the parameter D simply adjusts the time versus length scales in the problem. Thus, one could set $D := 1$ by simply adjusting α (which has units of time/(space)^2, as does $1/D$). Within this scaling, the latent heat, ℓ, has been incorporated into the dimensionless

temperature so that the coefficient of v in (1.2') is unity. For the limiting situations such as Hele-Shaw in which latent heat approaches zero one must adopt a scaling such as (1.1)-(1.3) which avoids division by ℓ.

The oldest mathematical model for an interface between two phases, e.g. liquid and solid, is known as the classical Stefan model which incorporates heat diffusion, (1.1) and the latent heat due to fusion, (1.2). Furthermore it stipulates that the interfacial temperature remains at the melting temperature [i.e. $u = 0$ replaces (1.2)]. This last condition, amounts to setting $\sigma = 0$ in (1.3) or $d_0 = 0$ in (1.3'). Although the capillarity length, d_0, is often very small compared to the other length scales in the problem, such as κ^{-1}, it is nevertheless very significant as a stabilizing force [Ch].

The classical Stefan model's neglect of surface tension and surface kinetics can be partially remedied by the imposition of (1.3) with finite σ and α. The numerical study of the surface tension and kinetics model [(1.1) - (1.3)] then becomes even more challenging as a consequence of the curvature term in (1.3).

Another sharp interface problem which arises in the context of a fluid between two plates is the Hele-Shaw model which can be expressed as equations [(1.1) -(1.3)] with the left hand side of (1.1) set at zero. For the Hele-Shaw problem, u describes pressure and the constants ℓ, κ, etc. represent different physical quantities (see [Oc], [Cr] and references contained therein).

Finally, one may consider the Cahn-Allen model of motion by mean curvature problem [AC], in which the interface moves with normal velocity

$$v = \frac{-1}{\alpha}\kappa \tag{1.4}$$

at each point on the interface $\Gamma(t)$.

Anisotropy may be considered in all of the problems above. In typical materials the anisotropy is present in the surface tension σ, and in the kinetic coefficient α so that (1.3') becomes

$$u = -d_0(\theta)\kappa - \alpha(\theta)d_0(\theta)v \tag{1.5}$$

where α is now a function of the orientation angle θ, and

$$d_0(\theta) := \frac{\sigma(\theta) + \sigma''(\theta)}{[s]_E \ell} c_{spm} \tag{1.5'}$$

The term $\beta(\theta) := \alpha(\theta)d_0(\theta)$ is often called the mobility (see [Ta] for general discussion). The orientation angle θ, may be defined as the angle between the normal to the interface and a fixed direction, or the angle between a fixed direction and the line from a central point to a point of the interface.

The precise nature of anisotropy and its interaction with undercooling (liquid below the equilibrium freezing temperature) is important in determining the shape of the interface, and one can obtain both a single needle crystal and cubic crystal growth from a cubic symmetry (see Section 5 for details).

Another approach to free boundary problems involves the use of a phase or "order" parameter, <t>, which specifies the phases ((^ ^2 1 is liquid, <p sc —1 is solid) while the level set *if* = 0 is now the interface. This approach has its origins in Landau theory [LL], Cahn-Hilliard type equations [CaHi], [La], and the application of mean field theory to critical phenomena [HH].

Phase field theories are generally rooted in the idea that each molecule or "spin" is under the influence of all others which effectively constitute an average "field" of interactions. This, of course, is a vast simplification over evaluating the sum over all possible states to calculate the partition function and, thereby, the free energy. Preliminary reports on a system of equations closely related to those discussed here (but with a different scaling which does not precisely attain any of the sharp interface models defined above) include **[Ca], [F].**

The variable *tp* represents the mean field or "averaged" description of the phase at each point (<,x) in time-space. This mean field approach has been used with some, but not complete, success in the subtle area of equilibrium critical phenomena. The application to ordinary phase transitions is actually quite different in that the correlation length (i.e. mean distance of which molecules Eire "aware" of one another's presence) is very small whereas it is very large in the critical region. In fact, the large correlation length provided the original justification for this approach. (See references in [Ca2] for further discussion.) Another difference between the critical region and ordinary phase transitions is that critical phenomena can rely on universality which states that the critical exponents should be independent of the details of the system. For solidification, it is generally desirable to specify all material parameters and to obtain quantitatively reliable results.

Using the scaling introduced in [Cal] we write the phase field equations in the form

$$c_{apm}T_t + i\leq p_t = \frac{K}{p}\dot{A}T \qquad \textbf{(1.6)}$$

$$\alpha\epsilon^2\varphi_t = \epsilon^2\Delta\varphi + \frac{1}{2}(\,?\,-\,¥\,>\,) + \frac{\epsilon}{3\sigma}(T-TE) \qquad (1\text{-}7)$$

where *e* is a parameter which is a measure of the interface width, and all other constants are as defined earlier. In 1985 it was shown [Cal] using asymptotics that the major free boundary problems could be attained as distinguished limits of the phase field equations in the form [(1.6), (1.7)]. In particular, if c approaches zero while all other parameters including *a* are held fixed, then the asymptotic solutions of [(1.6), (1.7)] are governed to leading order by the surface tension and kinetics model [(1.1)-(1.3)].

The classical Stefan model can be similarly recovered in the distinguished limit as *both t* and *a* vanish with *e/a* —> 0. The formal asymptotics has been made mathematically rigorous in some cases of special symmetry such as travelling waves [CN] and general *Id* and radially symmetric [CC]. Other important free boundary models such as the Hele-Shaw equations and motion by mean curvature are also obtained from the phase field equations (Ca2j.

Using the variables defined before [(1.1') - (1.3')] the equations [(1.6)-(1.7)] can be written in the form

$$u_t + \frac{1}{2}\varphi_t = \mathrm{DA}\,u \qquad (1.6')$$

$$\alpha\epsilon^2\varphi_t = \epsilon^2\Delta\varphi + \frac{1}{2}(\varphi - \varphi^3) + \frac{\epsilon}{3d_0}u \qquad (1.7')$$

With d_0 and/or α possibly depending on θ, the solutions of $[(1.6'), (1.7')]$ approach those of $[(1.1'), (1.2'), (1.5)]$. In a philosophical sense this approach to solidification computation problems is similar to artificial viscosity methods [PT] in gas dynamics in that the success of the method depends on whether the interface development is independent of ϵ for some range $(0, \epsilon_0)$.

The boundary conditions imposed on $[(1.6'), (1.7')]$ are the same as the sharp interface problem for u, with compatible conditions for φ. In particular, if one imposes Dirichlet conditions $u = u_{\partial\pm}$ then the corresponding values of φ are the roots of

$$\frac{1}{2}(\varphi_\pm - \varphi_\pm^3) + \frac{\epsilon}{3d_0}u_{\partial\pm} = 0 \qquad (1.8)$$

where the plus and minus denote the liquid and solid portions of the boundary, respectively.

In this paper we discuss the numerical study of the phase field equations with the aim of demonstrating that single system of equations can be used to compute a broad spectrum of phenomena which are generally associated with the sharp interface problems defined above. The advantages of the phase field model include the following. (A) The variety of phenomena ranging from motion by mean curvature to stable anisotropic cyrstal growth to single-needle dendrites are all obtained by simply varying parameters. (B) The system of equations has smooth solutions and does not involve explicit conditions on the interface. Hence, the interface is simply the level set $\varphi = 0$ and interface tracking is not required. (C) All of the physical parameters are clearly identified so that the system can be used to obtain quantitatively reliable numbers. (D) Computations involving self-interactions of the interface do not pose difficulties for the phase field model.

To illustrate how intersections create problems, we consider the following example. Two solid spheres with a small space between them are surrounded by the liquid which is undercooled so that the spheres grow slowly. At some point the spheres touch and begin to solidify together. If one models this situation using [1.1)-(1.3)] then there is the appearance of a mathematical singularity due to (1.3) when the spheres touch. This is a mathematical artifact, however, as the equation (1.3) is not a physically complete description of the interfaces in this complex situation , since condition (1.3) has not been defined when the classical normal is not defined. On the other hand, the phase field equations are guaranteed to have a smooth solution (φ, T) if the initial and boundary conditions are sufficiently smooth. Thus, the phase field model naturally describes the evolution of intersecting interfaces, such as this example, as it is based on a free energy description of the phases rather than a macroscopic derivation for a particular (smooth) geometry. The situation may be summarized by stating that the sharp interface problems such as [(1.1)-(1.3)] or (1.4) are a macroscopic approximation for simple geometries, so that a discrepancy between these models and the phase field is generally resolved by noting that the sharp interface model is not a correct approximation for the physical problem when the conditions for their derivation are no longer valid.

The numerical study of equations [(1.6), (1.7)] must confront the issue that the true physical size of ϵ (which is of the order of the width of the interface) is about 10^{-8} cm

while the overall domain of interest may vary between 10^{-1} cm for dendritic growth and 10^2 cm for casting of metals. Since the grid spacing cannot be significantly smaller than ϵ without large errors [CS1,2], a simple application of the phase field equations with physical parameters would imply a grid of at least $10^7 \times 10^7$ for dendritic growth and $10^{10} \times 10^{10}$ for casting for example. This grid size is prohibitive for practical computations. With this motivation [CS1,2] studied the ansatz that ϵ can be made orders of magnitude larger (i.e. the interface can be spread) within the limitations (a) and (b) below, without significant error, provided that this stretching is done within the proper scaling limits [Ca1,2] so that the crucial quantities such as the surface tension are not altered even by a small amount. The two key restrictions are that: (a) ϵ must be smaller than the radius of curvature; (b) ϵ cannot be large enough to destroy the double-well nature of the potential $\frac{1}{2}(\varphi - \varphi^3) \pm \frac{\epsilon}{3}\frac{1}{d_0}u$. The restriction (b) is easily remedied with a modification such as that introduced in [CC] where u is multiplied by a factor $(1-\varphi^2)^2$ or a similar function. This has the effect of trivializing the role of temperature outside of the interfacial region where it is usually very small. On the other hand restriction (a) is fundamental and is intrinsic to the physical problem. In particular, independent of the specific method, one does not expect to resolve an interface with a radius of curvature, R, by means of a mesh spacing, Δx, which is greater than R. Within this natural limitation, [CS1,2] showed that quantitatively reliable calculations could be performed using the equations [(1.6)-(1.7)].

In particular, [CS1,2] studied the one-dimensional and radially-symmetric equations corresponding to [(1.6), (1.7)], and compared the computations with the exact solutions for the limiting sharp interface problem and examined them through self-consistency. Subject to the radius of curvature limitation, it was established that the interface could be stretched by orders of magnitude without significant loss of accuracy, even in physically delicate situations. On the other hand, even a 10% change in surface tension resulted in dramatic changes in the evolution of the interface.

In the current paper, our primary aim is to show that in two-dimensions a range of sharp interface problems with distinct patterns can be computed using the phase field equations. A secondary objective is to verify that the interface can be stretched with quantitative accuracy when the computations are truly higher dimensional (instead of radially symmetric equations). In the higher dimensional case, the issue of interface stability is also relevant so that enlarging ϵ is predicated on the expectation that it does not significantly alter stability properties. We confirm this in both the planar and spherical cases, and, again use self-consistency and comparison with exact solutions.

We begin by considering planar travelling waves for the phase field equations within the modified Stefan limit. Since the velocity of the travelling waves for the sharp interface problem is known [CCh] from the analytic solution, we compare our computations with the exact results. The travelling wave is then perturbed with a sine wave so that the stability properties can be examined in the context of the sharp interface problem. We find that a typical unstable mode in the sharp interface problem is also unstable in the phase field equations.

In Section 3 we consider the problem of the critical radius, which is an unstable equilibrium in solidification [Ch] and obtain quantitative agreement with the analytical results. Anisotropic surface tension is then considered as we observe the change in interface shape

as a function of both equilibrium and dynamical anisotropy. In equilibrium, these results can be compared with well established results such as the Wulff construction approach [Wu,Ta,CH].

In Sections 4-6 we demonstrate that a broad spectrum of sharp interface problems can be approximated by the phase field model in the distinguished scaling limits as indicated in [Ca1,2]. Section 4 features the limit of motion by mean curvature in which the interface is often characterized by reduction of curvature by becoming more circular, and then shrinking until extinction. The extinction time from a circle is readily calculated analytically so that quantitative agreement of the numerical computations is verified along with the qualitative.

In Section 5 we consider solidification in the case of the single needle crystal. The computations result in a single needle which moves at essentially constant velocity. Furthermore, this velocity is independent of the initial conditions. This is consistent with the known experimental [GS,SG] and theoretical [BP,L,KKL] results.

Finally, in Section 6, we consider solidification under conditions which favor more stable growth, so that the faceted crystal growth is observed in the anisotropic situation. It is noteworthy that a completely smooth set of equations with smooth initial data render faceted shapes, e.g., cubic. The results obtained are consistent with those obtained from the classical Wulff construction methods.

Throughout this study we use finite difference methods ([CL], [CS2]) with a fixed grid in order to isolate the issues that are of specific interest. In principle, a combination of phase field methods and adaptive grids with finite elements should provide similar accuracy at a lower cost.

Some of the other numerical studies of solidification include [LF,SS,K,RT].

2. Plane fronts, stability and the emergence of single needle dendrites. We study first the travelling wave solutions for the phase field equations [(1.6), (1.7)], the existence of which was established in [CN]. Next, we perturb the planar fronts in order to examine the stability properties of the interface (for which there are no analytical results). In particular, we present the growth of needle type crystals from perturbations. These computations bridge the gap between the initial Mullins-Sekerka instability [MS] and the steady-state dendrites [PB] which evolve from them.

We consider the $(1.6'), (1.7')$ in the distinguished limit of the surface tension and kinetics model $(1.1') - (1.3')$, i.e. ϵ approaches zero with all other variables fixed. For the sharp interface problem, one can verify the existence [CCh], [DHOX] of the following travelling wave solutions with velocity v^* and $u(t,\infty) = u_{\text{cool}}$:

$$u(t,x) = \begin{cases} u_{\text{cool}} + e^{-v^*(x-v^*t)/D} & x > v^*t \\ u_{\text{cool}} + 1 & x \le v^*t \end{cases} \tag{2.1}$$

$$v^* = \frac{-1}{\alpha d_0}(u_{\text{cool}} + 1) \tag{2.2}$$

In order to ensure the positivity of the velocity v^*, one must assume

$$u_{\text{cool}} + 1 < 0. \tag{2.3}$$

Note that the velocity v^* and the temperature at the interface $u_{\text{cool}} + 1$ (and in fact for all x in the solid region, $x \leq v^* t$) are both determined by the temperature at ∞, i.e. u_{cool}. Also, the latent heat is just unity for our temperature scale.

In order to state the analogous problem for the phase field equations (1.6'), (1.7') one must impose conditions on φ as well as u. A natural set of conditions [CN] is

$$\varphi(-\infty) = \varphi^\epsilon_\infty \qquad \varphi(\infty) = \varphi^\epsilon_\infty \tag{2.4}$$

$$u(-\infty) = u_{\text{cool}} + 1 \qquad u(\infty) = u_{\text{cool}} \tag{2.5}$$

in terms of the moving coordinate $z := x - vt$ where v is to be determined. Here, the values $\varphi^\epsilon_{\pm\infty}$ must satisfy the compatibility condition (1.8).

In terms of the moving coordinates, the phase field equations have the form

$$\epsilon^2 \varphi_{zz} = \alpha \epsilon^2 v \varphi_z + \frac{1}{2}(\varphi - \varphi^3) + \frac{\epsilon}{3d_0} u = 0 \tag{2.6}$$

$$D u_{zz} + v(u_z + \frac{1}{2}\varphi_z) = 0 \tag{2.7}$$

It was proven in [CN] that there exist a unique solution of [(2.6), (2.7)] subject to (2.4), (2.5) for small ϵ, and the velocity v (which depends on ϵ) approaches v^* given by (2.2). The far-field temperature u_{cool} not only determines the velocity, but the other boundary conditions in (2.4) - (2.5) as well [CN]. In the limit of $\epsilon \to 0$, the temperature u in (2.6), (2.7) converges to the temperature (2.1) of the sharp interface model uniformly with respect to the distance measure given by the moving coordinate, z. Other analyses of travelling waves for phase field equations in other scaling limits have been performed in [Wi], [BS], [LBT].

An important question which is not resolved by the theoretical results is the rate at which the velocity $v(\epsilon)$ converges to v^* as ϵ approaches zero. Stated differently, the physically realistic value of ϵ is on the order of Angstroms, whereas in practical computations, one would need to make ϵ larger by orders of magnitude.

Hence our first goal is to determine if the computation of plane waves are still reliable in the above situation. If so, by taking values of ϵ which are small but still much larger than the true physical value, the front velocities and stability properties should not differ significantly from the velocity of the sharp interface model.

In our experiments we set the parameters to be $D = 1.0, \alpha = 1.0, d_0 = 0.01$ and $u_\infty = -1.05$, which yield a theoretical velocity $v^* = 5.0$. We then examined the nature of the convergence to the exact solution of the sharp interface model, by halving ϵ as shown in Table 1.

We perform the same computation with each value of ϵ, and examine the relative error of the interface,

$$\frac{x(\text{theoretical}) - x(\text{experimental})}{x(\text{theoretical})}$$

at a characteristic point ($t = 0.0051$). Note that while ϵ is cut in half between experiments 1 and 2, the relative error in the interface position is reduced to one-fourth. Similarly, the relative error in velocity is reduced from 0.543 for $\epsilon = 0.00495$ to 0.093 for $\epsilon = 0.00247$. Between experiments 2 and 3 the relative error in the interface is similarly reduced. Since the approximations used in determining velocity are less accurate than those of the interface, there appears to be a finite limit to the relative error in velocity.

TABLE 1: RELATIVE ERROR WITH DIFFERENT VALUES OF ϵ

	ϵ	Relative Error In Interface at $t = 0.0051$	Relative Error In Velocity at $t = 0.0051$	Maximum Relative Error In Velocity
# 1	0.00495	0.162	0.543	0.911
# 2	0.00247	0.048	0.093	0.353
# 3	0.00124	0.015	0.081	0.153

In an earlier work [CS1,2], we studied plane fronts in the distinguished limit of the classical Stefan model (there are no travelling waves in this case), using a one-dimensional formulation. The significant difference between one and two-dimensional computations necessitate the testing of plane fronts and travelling waves in the actual two spatial dimensions. In our $2d$ experiments, we reproduced the exact classical Stefan results with a relative error of 0.0008 with 200 mesh points and $\epsilon = \Delta x$. The two sets of computations ($1d$ and $2d$) agreed to the first 12 digits, thereby confirming the absence of extraneous grid effects in $2d$.

Hence, our basic conclusions for the $1d$ travelling waves [CS1,2] in the surface tension and kinetics limit remain valid within the $2d$ context. The overall φ profile is essentially identical with the $1d$ calculations. The boundary conditions $\varphi_\pm$ are determined by (2.4) in correspondence with (1.8). The φ-level curves are all parallel to the interface and φ is approximately given by the function $\tanh(\frac{x-vt}{2\epsilon})$ as indicated by the theoretical results [CN]. The transition layer is thus $\mathcal{O}(\epsilon)$ as in the $1d$ case. More specifically, if we take $\varphi = \pm.9$ as the cutoff in the transition layer then the transition layer has a width 6ϵ; for cutoff $\varphi = \pm.99$ it is 10ϵ. Of course, we know from the theoretical results that the order ϵ correction to φ is crucial in the selection of the interface velocity, so that a correct interface velocity is confirmation of the order ϵ φ profile.

It is also noteworthy that the numerical error does not cause shape instability of the planar front, unlike the perturbation discussed below. This is consistent with the phase field theory since the stability properties of the [(1.6), (1.7)] are the same as those of [(1.1) - (1.3)] to leading order [J] and the latter can be expected to be stable for perturbations with wavelengths which are on the size of the mesh used. The precise conditions are given in [CCh] and [J].

Next, we consider a planar wave whose interface is perturbed by a sinusoidal function, so that the interface location is given by

$$x(y) = a + b \cos my$$

The parameters and boundary conditions, remain the same as in experiment 1 with the initial temperature set $u_\infty + 1$ in the solid and exponential decay to the boundary in the x-direction.

In Figure 2.1 we show snapshots of the time evolution of the interface at $t = 0.0$, 0.00367, 0.00826, 0.01286, 0.01745, 0.022041, 0.03122. In this experiment $m = 1, a = 0.21$ and $b = 0.1485$. It can be clearly observed how the initial perturbation evolves into a needle type shape.

Hence, the development of instabilities where one expects them on physical and theoretical grounds, and the absence of extraneous instabilities due to numerical error indicate the suitability of using phase field equations to study interfaces.

It was noted in [CS1,2] that there are questions of optimization in choosing ϵ with respect to the mesh spacing, Δx. For a fixed grid, practical constraints impose a lower bound on Δx. For a fixed Δx, the question of the optimal choice of ϵ is more subtle. If ϵ is too small compared to Δx, then the surface tension, which is proportional to $\int (\nabla\varphi \cdot n)^2 dx$, will not be calculated accurately since there will be too few grid points in the interfacial region. This is easily illustrated with the tanh function which approximates φ, so that surface tension is essentially proportional to $\int \text{sech}^2(r/2\epsilon)dx$. Recalling that the transition layer is about 6-10 ϵ, depending on the precise cutoff point, a grid spacing of about $\Delta x = \epsilon$ would result in 6-10 grid points on the interfacial region. Clearly, any fewer than 6 points would mean that the surface tension is not accurately computed. Since surface tension is crucial for the stability properties of the interface and this integral also has a key role in determining the $\mathcal{O}(\epsilon)$ terms in the solution, this is an important constraint.

Alternatively, if ϵ is too large then (a) it diffuses the interface so that geometries with radii of curvatures smaller than ϵ would not be captured, and (b) the $\mathcal{O}(\epsilon)$ dynamics becomes a more significant factor limiting the quantitative accuracy of the interface velocity, as indicated by the asymptotic analysis.

In the two-dimensional problems we found the optimal value of the ratio $\epsilon/\Delta x$ to be $0.75 \leq \epsilon/\Delta x \leq 1.1$, as in the $1d$ problems. This is not very surprising in view of the asymptotic analysis, in which the size of ϵ is significant primarily in the direction perpendicular to the interface.

For the remainder of this paper we will use the ratio $\epsilon/\Delta x = 1$. Performing the same empirical optimization in some of the low symmetry examples implies a similar range for $\epsilon/\Delta x$.

The computation in Figures 2.1, 3.1, 4.1, 5.1, 6.2, 6.3 were done using a CRAY YMP with 200 mesh points per side. Computations performed with 400 mesh point were very similar though much more costly. We use the same type of explicit schemes as in [CS1,2] and similar time scales. The time step in all cases is the largest allowed by numerical stability considerations. The numerical runs continued until complete solidification or melting.

3. The Critical Radius and Unstable Equilibrium. A well-known instability in materials science is the critical radius ([Ch] p. 67) in which a solid sphere with the sum of principal curvatures equal to AC_0 is in equilibrium with its melt at temperature UQ with

$$u_0 = -d_0 / c_0 \tag{3.1}$$

Under suitable conditions, e.g. Dirichlet boundary conditions and, £, A""[1] sufficiently small, a perturbation of the sphere to a larger one results in complete solidification and analogously for melting (see [CS2] for more discussion). The numerical computations assuming spherical symmetry confirmed this unstable equilibrium and showed that a small change in K or a produces a dramatic difference (melting to freezing or vice-versa) while a large change in c only produces a small change in velocity.

We study this problem now in the fully two dimensional geometry (without imposing spherical symmetry), and find that the spherical geometry is preserved. The values of A*,£, etc. are identical to those reported in [CS2] and again there is a 12-digit agreement between the one-dimensional and two-dimensional results for the location of the interface. Again, this confirms the absence of artificial grid effects.

Thus, the two dimensional calculations confirm the existence of this physical instability without causing artificial numerical instabilities nor necessitating the use of explicit equations of motion for the interface. Furthermore, in Figure 3.1 we illustrate the results obtained when the initial interface is the perturbed circle r = 0.3(1 + (cos80)/3). The parameters correspond to a critical radius ro = 0.01732, and as predicted by equation (1.5) the interface evolves to a spherical shape and continues to freeze.

The introduction of anisotropy with respect to a fixed angle in the surface tension changes (3.1) into

$$\kappa_0 = -[s]_E u_0 / (\sigma(\theta) + \sigma''(\theta)) \tag{3.2}$$

This expression for the curvature implies that the equilibrium shape is a dilation of the Wulff region. Figure 3.2 depicts the Wulff crystal for pivalic acid. This will be discussed in greater detail within the context of crystal growth in Section 5.

The *2d* computations on the critical radius and the perturbed circle (Firgure 3.1) axe also useful in demonstrating that grid effects do not introduce artificial anisotropy. In particular, the grid effects would be most pronounced for the critical radius problem since the initial configuration is borderline between melting and freezing, so that any extraneous effects would be magnified.

4. **The single-needle crystal.** In Sections 4-6 we use the phase field equations to study a spectrum of problems which involve different physical parameters and behavior. One set of numerical experiments (see Figures 3.1. 4.1, 5.1, 6.3) are performed with identical initial conditions in order to illustrate the wide range of applicability.

The first of these is the single-needle crystal solidification at high velocities. Anisotropy is generally regarded to be important for this problem as both a and a vary with respect to orientation angle, 0. A series of physical experiments [SG, GS] indicate that the role of anisotropy is to select the direction of the growth rather than to determine the shape

or velocity of the tip. are not as pure as [GS]. For example, the extent of anisotropy in the surface tension is 10 times greater for pivalic acid than succinonitrile, yet the shape and dimensionless velocity (as a function of undercooling) are essentially idential [GS.] However, other measurements suggest that the anisotropy of these materials is closer than that by [SG, GS]. These measurements are for samples which are not as pure as [GS]. In an earlier work [CL] the anisotropy in σ has been studied. In these numerical experiments, we study the effects of dynamic anisotropy, which is not as well understood in terms of the physical experiments. As a precise physical form for dynamical anisotropy has not been established, we use a (phenomenological) function which is strongly anisotropic along the diagonal. In particular

$$\alpha^{-1} = \begin{cases} \alpha_0 + (1-\alpha_0)(\cos\frac{4\pi}{\sqrt{2}}d)^4 & \text{if } \frac{-\sqrt{2}}{8} < d < \frac{\sqrt{2}}{8} \\ \alpha_0 & \text{otherwise} \end{cases} \tag{4.1}$$

where d is the distance to the diagonals (between $\hat{x}$ and $\hat{y}$ axes). Note that the dynamic anisotropy will not generally have a form such as (1.5′), which arises from the second derivatives in the Laplacian.

In a part of the interface in which the temperature and curvature does not vary significantly, the velocity is given by

$$v \cong -\alpha^{-1}(\text{const}) \tag{4.2}$$

so that the diagonal is the preferred direction of growth. Figure 4.1 displays a time sequence in which the initial condition is a circle which is strongly perturbed by a sine function with values of $\alpha_0 = 0.1$. The growth is chiefly in the preferred direction. The diagonal was chosen as the preferred direction in order to ensure that anisotropic growth would not be the result of grid effects. In fact, the absence of anisotropic growth when α^{-1} is isotropic indicates that grid effects are not significant.

There is considerable experimental [SG, GS, DG], and theoretical evidence [BP, LKK, L] which suggests that the velocity of the single-needle should be constant. This is confirmed by our numerical experiments, even though only linear interpolation is used to determine both the interface location and its velocity.

Furthermore, this velocity is found to be independent of the initial conditions which is consistent with the experimental and theoretical results cited above. Figure 4.2 depicts the convergence to a selected velocity from distinct initial conditions. The velocity, 44.13, is constant to within 0.62%.

5. Faceted Crystal Growth. The geometric patterns and facets which arise from crystal growth have posed intriguing questions for many years. A very early scheme to describe the equilibrium interface is known as the Wulff construction [Wu], which will be described later in this section. The propagation of facets and the development and elimination of corners has been studied extensively in recent decades from the minimal surfaces and related approaches [Ta].

In such studies, the corners are explicitly part of the numerical scheme. The evolution of faceted crystal growth poses a particularly strong challenge for a smooth set of parabolic equations, such as the phase field. Given a smooth initial data (e.g. first frame of Figure 5.1) a material with anisotropy must eventually develop corners and facets and must propagate along planar fronts dictated by the geometry and anisotropy.

The anisotropy in the phase field equations can involve both $\alpha(\theta)$ and $\sigma(\theta)$ where θ is now defined to be the angle between the normal to the interface and the x-axis, i.e.

$$\cos\ \theta = \frac{\nabla\bar{\varphi}}{|\nabla\varphi|} \cdot \hat{x} \tag{5.1}$$

We study the anisotropy by assuming σ and/or α are of the form

$$\sigma(\theta) = \sigma_0[1 + \delta_\sigma \cos\ M(\theta - \theta_\sigma)] \tag{5.2}$$

$$\alpha^{-1}(\theta) = \alpha_0^{-1}[1 + \delta_\alpha \cos\ M(\theta - \theta_\alpha)] \tag{5.3}$$

where M is an integer ($M = 4$ for cubic anisotropy), $\delta_\sigma, \delta_\alpha \in \mathbb{R}^+$ are the amplitudes of the anisotropies and $\theta_\sigma, \theta_\alpha$ are the "preferred" angles. The latter will be defined more precisely below.

The phase field equations we study are then (1.6′), (1.7′) with d_0 and α given by (1.5′), (5.2), (5.3). In the asymptotic limit as ϵ approaches zero, the solutions to these phase field equations are governed to leading order by those of [(1.1′), (1.2'), (1.5), (1.5′)]. Since these dimensionless equations are related to the fully dimensional equations by simple substitution, every parameter in our system including those involving anisotropy, e.g. δ_σ, can be obtained directly from experimental data. Of course we wish to "stretch out" the parameter ϵ, as discussed earlier, for computational convenience.

Next, we consider the issue of preferred direction, which is similar for the phase field and sharp interface models, in view of the remarks above. Consider the sharp interface problem [(1.1′), (1.2'), (1.5), (1.5′)] in equilibrium so that temperature is constant. Then (1.5) (1.5′) implies (for some constant C^2)

$$\kappa = \frac{C^2}{\sigma(\theta) + \sigma''(\theta)} \tag{5.4}$$

$$\sigma(\theta) + \sigma''(\theta) = \sigma_0[1 - (M^2 - 1)\delta_\sigma \cos\ M(\theta - \theta_\sigma)] \tag{5.5}$$

Hence, if we assume δ_σ satisfies $(M^2 - 1)\delta_\sigma < 1$ then the curvature has its maximum when $\theta = \theta_\sigma$. For cubic anisotropy ($M = 4$) with $\theta_\sigma := \pi/4$ this means that the equilibrium shape of the interface is such that the solid protrudes further in the diagonal directions.

This brief illustration is one implication of the Wulff construction [Wu] and can be obtained from the Cahn-Hoffman [CH] $\bar{\xi}$ vector approach or the Herring spheres approach. Note that when $\sigma + \sigma''$ changes sign, then one has facets in the equilibrium shape as a

consequence of missing angles or orientations. The values of 6_a for two materials used in dendritic experiments are 0.05 for pivalic acid and 0.005 for succinonitrile [GS].

The dynamical situation is more complicated even if the kinetic term *ado* in (1.6) is neglected completely. On the other hand, in a limiting case in which curvature is neglected and a ^ 0 , one can acquire a basic understanding of the effects of this kinetic term. This analysis amounts to a comparison of velocities of planar fronts with different orientations, so that (1.5), (1.5') imply

$$v \approx \frac{C^2}{a\{8)[*\{0) + *''(\theta)]} \qquad (5.6)$$

Once again, for small S_a and £a, and $6^* = \$_Q$, the velocity is maximum at $6 = 6_9 = 6_Q$. Hence, in the cubic case (M = $A,8_a = 6_Q$ = TT/4) the growth is fastest in the diagonal directions.

These two calculations illustrate the following expectations. An initially spherical solid with cubic anisotropy will tend to grow fastest in the diagonal directions. If the boundary conditions are such that equilibrium is reached (e.g. appropriate Neumann conditions) then the interface will correspond to the WulfF shape which is shown in Figure 3.2, i.e. a square with rounded corners. Note that while the equilibrium result (5.4) is exact, the dynamic result (5.6) is only suggestive since the temperature will not be exactly constant and curvature is not precisely zero. Furthermore, one has a natural expectation that the dynamics will be less stable than equilibrium, thereby exaggerating growth in the favored directions. Thus, it is possible that the dynamical problem will have facets for smaller anisotropies than those required by the vanishing of the denominator of (5.6) which would be the condition for "corners" or missing angles in equilibrium according to the WulfF construction.

While we consider the usual case in which $6_a = 6_Q$ it is worth noting that some materials exhibit dynamical anisotropy with a different preferred direction than that of the equilibrium.

In our numerical computations, we study a material with anisotropy given by (5.2) or (5.3) (with h_a = 0.05 or 6_Q = .818 and M = 4 and 6_a = TT/4 or 6_Q = TT/4.). Note that the dynamic anisotropy appears to be larger but the coefficient of 6_{ff} is multiplied by M^2 — 1 = 15. Our value of 6_a corresponds exactly to that reported by [GS] for pivalic acid. The computations show that a material with such anisotropy will evolve into a shape with four-fold symmetry, regardless of the initial pattern. In particular, Figure 5.1 displays 12 frames in the phase field computations [(1.6'), (1.7')] using (5.3) (i.e. with $d_o(6)$ defined by (1.5'). Similar results are obtained with (5.2). The fact that such different sources of anisotropy [(5.2) versus (5.3)] result in very similar patterns is an important physical conclusion which is not obvious from the form of the equations. The initial shape is the same perturbed circle used in the formation of the single needle dendrite. By frame 3, this interface develops some corners and facets, some of which correspond to the favored directions discussed above, while others form as an immediate consequence of the initial conditions. In frames 3 - 9 these latter facets axe gradually eliminated at the expense of the dominant facets distinguished by (5.4) and (5.6). In the last few frames (i.e. 10 -

12) these dominant planes become extended until they meet at the $x-y$ diagonal with a slightly smoothed out right angle. The solidification then continues without any change in shape.

A rigorous result [So] has established that an interface moving in accordance with (1.3′) alone, with constant u, would retain the anisotropic shape. While there are no rigorous results for the full set of equations involved in solidification, our numerics show that this is indeed the case for the phase field equations. Since these equations are asymptotically governed by (1.1′) - (1.3′) to leading order, the same conclusion remains valid for the sharp interface problem.

6. Motion by Mean Curvature. The problem of motion by mean curvature (see [Br] and references contained therein) is to determine a $(d-1)$-dimensional surface (or curve) $\Gamma_s(t)$ in $\Omega \subset \mathbb{R}^d$, such that the (normal) velocity, $v(t,x)$, at each point on the surface satisfies

$$v(t,x) = -\alpha^{-1}\kappa(t,x) \tag{6.1}$$

where κ is again the sum of principal curvatures and α^{-1} is a constant or a function of orientation angle.

A closely related problem is to find that the level set

$$\Gamma(t) := \{x \in \Omega : \varphi(t,x) = 0\} \tag{6.2}$$

where φ is a solution to the single parabolic equation

$$\alpha\epsilon^2\varphi_t = \epsilon^2\Delta\varphi + \frac{1}{2}(\varphi - \varphi^3) \tag{6.3}$$

Equation (6.3), which was introduced by Cahn and Allen [CA][AC] in the context of antiphase boundaries is a limiting case of the phase field equations. As the latent heat, ℓ, approaches zero while the initial and boundary conditions imposed on u are also zero, the phase field equations [1.6′), (1.7′)] have solutions which are governed by those of (6.3) and consequently (6.1) to leading order. Thus, the leading order asymptotics for [(1.6′), (1.7′)] is just a special case of (1.5) in which $u = 0$ [Ca2]. In recent years, the connections with materials science through the phase field equations have stimulated a resurgence of interest in the mathematical theory of equation (6.3) and other regularizations of (6.1). From a formal analysis it is clear that an initial interface of the form of frame 1 in Figure 6.3 will tend to approach a circle and then shrink until extinction. The time of extinction from a cricle is easily calculated. Rigorous theorems have established these results under general conditions [So].

Our numerical calculations consist of studying [(1.6), (1.7)] in the limit of small ℓ, with zero boundary and initial conditions for u and the standard conditions of φ described in (2.10) so that $\varphi_+ = +1$ on the (exterior) liquid and $\varphi_- = -1$ in the (interior) solid in this case. In our first experiment we compared the numerical results with a theoretical solution. We took $\alpha = 1, \ell = 0$, zero boundary and initial conditions for u, and the initial solid seed to be a circle of radius 0.3. The theoretical solution gives a circle with radius $r(t) = (0.09 - 2t)^{1/2}$ which has an extinction time $T_0 = 0.045$.

In Figure 6.1 we depict the computed and theoretical radius of the circle as a function of time. There is an agreement of two or more digits up to $t = 0.0345$ and the accuracy deteriorates approaching T_0. The computational extinction time is between 0.04575 and 0.0465. Figure 6.2 depicts the evolution at times

$$t = 0.0, 0.00675, 0.01425, 0.02175, 0.02925, 0.03675$$
$$0.04425, 0.04565, 0.0465.$$

The initial condition in frame 1 of Figure 6.3 is identical to those which we used for faceted crystals and stable solidification. In frames 1 - 4 the interface moves toward a circle (frame 5) with a radius which is approximately that of the perturbed circle in frame 1. The interface acts in a way to minimize the surface tension during this phase. The surface tension in (6.3) or (1.7) is determined to leading order by the coefficients of $\Delta\varphi$ and the $\frac{1}{2}(\varphi - \varphi^3)$ term.

The anisotropic analog of (6.1) involves replacing the constant α by a function of orientation angle as discussed earlier in the single needle or faceted crystal growth cases. Note that the anisotropy involved in the surface tension is not relevant in this limit since σ cancels in the asymptotics. In the anisotropic case the evolution of the interface is similar except that the convergence of the interface is toward the appropriate Wulff shape rather than the sphere.

Acknowledgements: The authors thank the Pittsburgh Supercomputing Center for computing time and use of facilities.

REFERENCES

[AC] S. Allen and J. Cahn, *A microscopic theory for antiphase boundary motion and its application to antiphase domain coarsening*, Acta Metall. **27** (1972), 1084-1095.

[BK] L. Bronsard and R. Kohn, *Motion by mean curvature as the singular limit of Ginzburg-Landau dynamics*, J. Diff. Eqns. **90** (1991), 211-237.

[BP] M. Ben-Amar and Y. Pomeau, Europhys. Lett. **2** (1986), 307.

[Br] K.A. Brakke, *The motion of a surface by its mean curvature*. Math Notes Princeton University Press.

[BS] M. Barber and D. Singleton, *Travelling waves in phase field models of solidification*, Preprint Australian National Univ..

[Ca] G. Caginalp, *The limiting behavior of a free boundary in the phase field model*, Carnegie-Mellon Research Report 82-5 (1982).

[Ca1] G. Caginalp, *Mathematical models of phase boundaries*, Material Instabilities in Continuum problems and related mathematical problems Heriot-Watt Symposium (1985-1986) (J. Ball, ed.), Oxford Science Publications, 1988, pp. 35-52.

[Ca2] G. Caginalp, *Stefan and Hele-Shaw type models as asymptotic limits of the phase field equations*, Physical Review A **39** (1989), 5887-5896.

[CC] G. Caginalp and X. Chen, *Phase field equations in the singular limit of sharp interface problems*, IMA Volumes in Mathematics and Its Applications **43** (1990).

[CCh] G. Caginalp and J. Chadam, *Stability of interfaces with velocity correction term*, Rocky Mtn. J. of Math. **21** (1991).

[Ch] B. Chalmers, *Principles of Solidification*, R.E. Krieger Publ., 1964.

[CH] J. Cahn and D. Hoffman, *A vector thermodynamics for anisotropic surfaces II. Curved and Faceted Surfaces*, Acta. Met. **22** (1974), 1205-1214.

[CHi] J.W. Cahn and J.E. Hilliard, *Free energy of a nonuniform system, I. Interfacial free energy*, J. Chem. Phys. **28** (1957), 258-267.

[CL] G. Caginalp and J. Lin, *A numerical analysis of an anisotropic phase field model*, IMA J. App. Math. **39** (1987), 51-66.

[CN] G. Caginalp and Y. Nishiura, *The existence of travelling waves for phase field equations and convergence to sharp interface models in the singular limit*, Quarterly of Applied Mathematics **49** (1991), 147-162.

[Cr] J. Crank, *Free and Moving Problems*, Oxford, 1984.

[CS1] G. Caginalp and E. Socolovsky, *Efficient computation of a sharp interface by spreading via phase field methods*, App. Math. Letters (1989), 117-120.

[CS2] G. Caginalp and E. Socolovsky, *Computation of sharp phase boundaries by spreading the planar and spherically symmetric cases*, J. Comp. Phys. **95** (1991), 85-100.

[DG] A. Dougherty and J. Gollub, *Steady state dendritic growth of N_4BR from solution*, Phys. Rev. A **38** (1988), 3043-3053.

[DHOX] J. Dewynne, S. Howison, J. Ockendon and W. Xie, *Asymptotic behavior of solutions to the Stefan problem with a kinetic condition at the free boundary*, J. Australian Math. Soc. Ser. B **31** (1989), 81-96.

[F] G. Fix, *Free Boundary Problems* (A. Fasano and M. Primicerio, ed.), Pitman, Boston, 1983, p. 580.

[GG] Y. Giga and S. Goto, *Geometric evolution of phase boundaries*, IMA Preprint # 738 (1990).

[Gl] J. Glimm, *The continuous structure of discontinuities*, Proc. of Nice Conference (Jan. 1988).

[GS] M.E. Glicksman and N.B. Singh, *Effects of crystal-melt interfacial energy anisotropy on dendritic morphology and growth kinetics*, J. Crystal Growth **98** (1989), 277-284.

[HH] P.C. Hohenberg and B.I. Halperin, *Theory of dynamics critical phenomena*, Reviews of Modern Physics **49** (1977), 435-489.

[J] J. Jones, Preprint in preparation, Univ. of Pittsburgh.

[K] R. Kobayashi, *Videotape and Preprint (1991)*.

[KKL] D. Kessler, J. Koplik and H. Levine, *Pattern selection in fingered growth phenomenon*, Adv. in Phys. **37** (1988), 255-339.

[L] J.S. Langer, *Lectures in the theory of pattern formation*, Chance and Matter (J. Souletie, ed.), No. Holland, 1987.

[LBT] H. Lowen, J. Bechhoefer and L. Tuckerman, *Crystal growth at long times...*, Simon Fraser Univ. Preprint.

[LF] J. Lin and G. Fix, *Numerical simulations of nonlinear phase transitions I. The isotropic case*, Nonlinear Analysis, Theory, Math. Appl. **12** (1988), 811-823.

[LL] J. Landau and E.M. Lifshitz, *Statistical Physics*, Addison-Wesley Publ, Reading, MA, 1958.

[MS] W.W. Mullins and R.F. Sekerka, *Morphological stability of a particle growing by diffusion or heat flow*, J. Apply. Phys **34** (1963), 323-329.

[MSc] P. Mottoni and M. Schatzman, *Geometrical evolution of developed interfaces*, Preprint (1989).

[Oc] J. Ockendon, *Linear and nonlinear stability of a class of moving boundary problems*, Proceedings of Pavia Conference, Free Boundary Problems (E. Magenes, ed.), 1980.

[PT] R. Peyret and T. Taylor, *Computational Methods in Fluid Flow*, Springer, Berlin (1983).

[RT] A. Roosen and J.E. Taylor, *Simulation of Crystal growth with faceted interfaces*, Preprint (1992).

[SG] N.B. Singh and M.E. Glicksman, *Free dendritic growth in viscous melts: cyclohexanol*, J. Crystal Growth **82** (1989), 534-540.

[So] H.M. Soner, *Motion of a set by the curvature of its boundary*, Preprint (1991).

[SS] J.A. Sethian and J. Strain, *Crystal growth and dendritic solidification*, Report PAM-509 Berkeley (1990).

[Ta] J.E. Taylor, *Motion of curves by crystalline curvature including triple junctions and boundary point*, Preprint (1991).

[Wi] J. Wilder, Univ. of West Virginia Preprint.

[Wu] G. Wulff, *Krystallograph*, Mineral **34** (1901), 499.

FIGURE CAPTIONS

Figure 2.1: Single needle crystal growth due to instability of a planar front. Initial interface at $x = 0.21 + 0.1485 \cos y$. Parameters are $D = 1.0$, $\alpha = 1.0$, $d_0 = 0.01$ and $u_\infty = -1.05$, which yield a Stefan planar front velocity $v^* = 5.0$.

Figure 3.1: Stability of permutations in the case of unstable equilibrium at critical radius. Initial interface at $r = 0.3(1 + \frac{1}{3}\cos\ 8\theta)$. Parameters are: $\alpha = 1.0$, $D = 1.0$, $\ell = 0.01$, $[s]_E = 4.$, $\epsilon = 0.005$ and $\sigma = 0.034651$ with critical radius $r_0 = 0.01732$.

Figure 3.2: Wulff crystal for pivalic acid.

Figure 4.1: Single needle crystal growth due to anisotropic mobility (4.1) with $\alpha_0 = .1$. Initial interface at $r = 0.3(1 + \frac{1}{3}\cos\ 8\theta)$. Parameters are $D = 1.0$, $\ell = 0.01$, $[s]_E = 4$, $\epsilon = 0.005$ and $\sigma = 0.034641$.

Figure 4.2: Needle crystal tip velocity convergence to a constant independent of initial interface. Initial interfaces at $r = 0.3$, $r = 0.3(1 + \frac{1}{3}\cos\ m(\theta - \frac{\Pi}{4}))$ and $r = 0.3(1 + \frac{1}{3}\cos\ m\theta)$ for $m = 4, 8$. Parameters are $D = 1.0$, $\ell = 0.01$, $[s]_E = 4$, $\epsilon = 0.005$ and $\sigma = 0.034641$.

Figure 5.1: Faceted crystal growth due anisotropic mobility $[\alpha^{-1} = .065(1 + 0.818\ \cos 4(\theta - \frac{\Pi}{4}))]$, is the angle between interface normal and x-axis. Initial interface at $r = 0.3(1 + \frac{1}{3}\cos\ 8\theta)$. Parameters are $D = 1$, $\ell = 0.01$, $[s]_E = 4$, $\epsilon = 0.005$ and $\sigma = .03464$.

Figure 6.1: Motion by mean curvature. Computed and theoretical interface locations for a circular initial interface. Exact radius is $r(t) = (0.09 - 2t)^{1/2}$ $0 \leq t \leq 0.045$. Parameters are $D = 1.0$, $\ell = 0$, $[s]_E = 4$, $\epsilon = 0.005$ and $\sigma = 0.866025$.

Figure 6.2: Motion by mean curvature. Cyrstal evolution corresponding to the computation of Figure 6.1.

Figure 6.3: Motion by mean curvature. Crystal evolution for initial interface $r = 0.3(1 + \frac{1}{3}\cos\ 8\theta)$. Parameters are the same as in Figures 6.1 and 6.2.

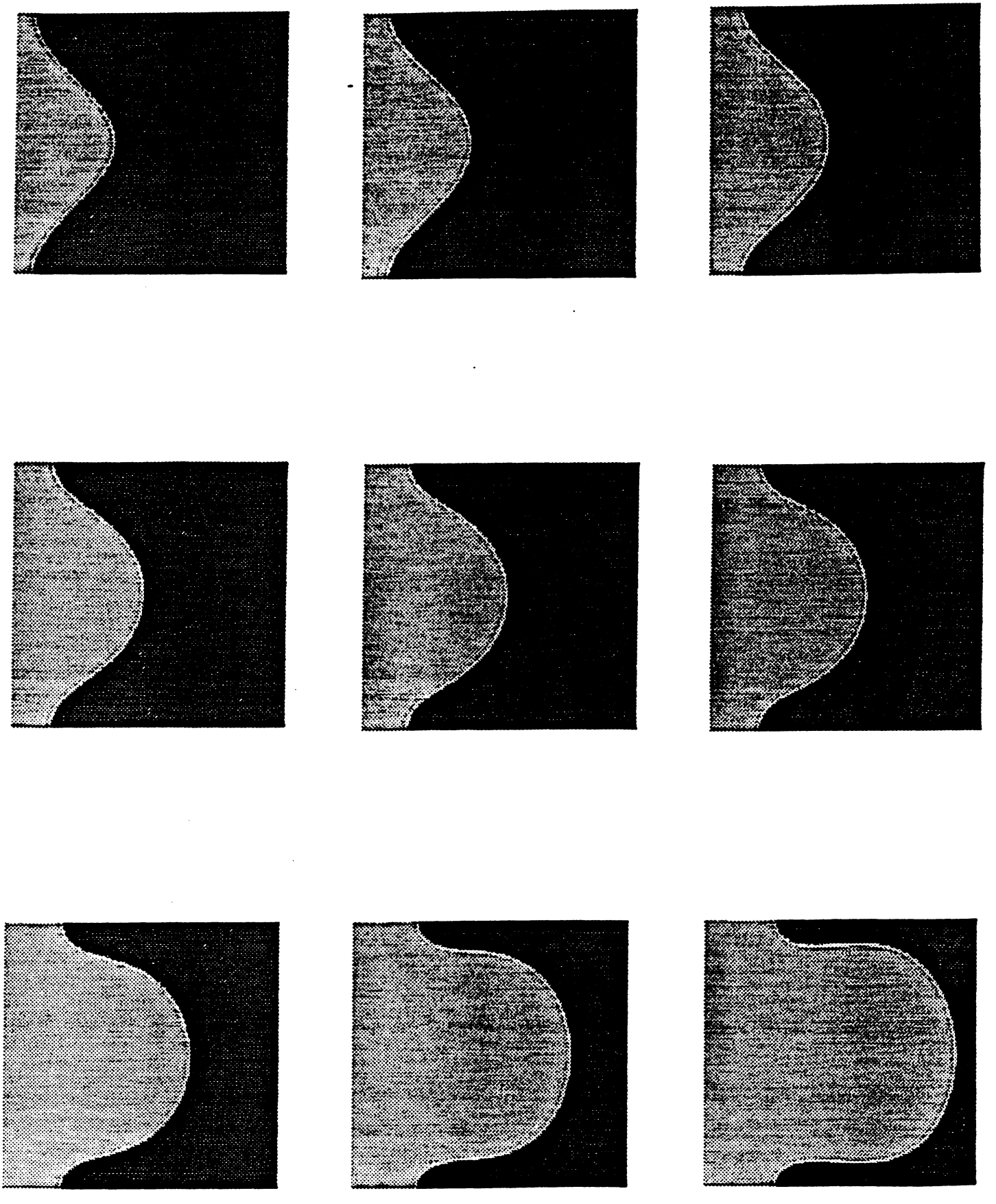

FIG. 2.1

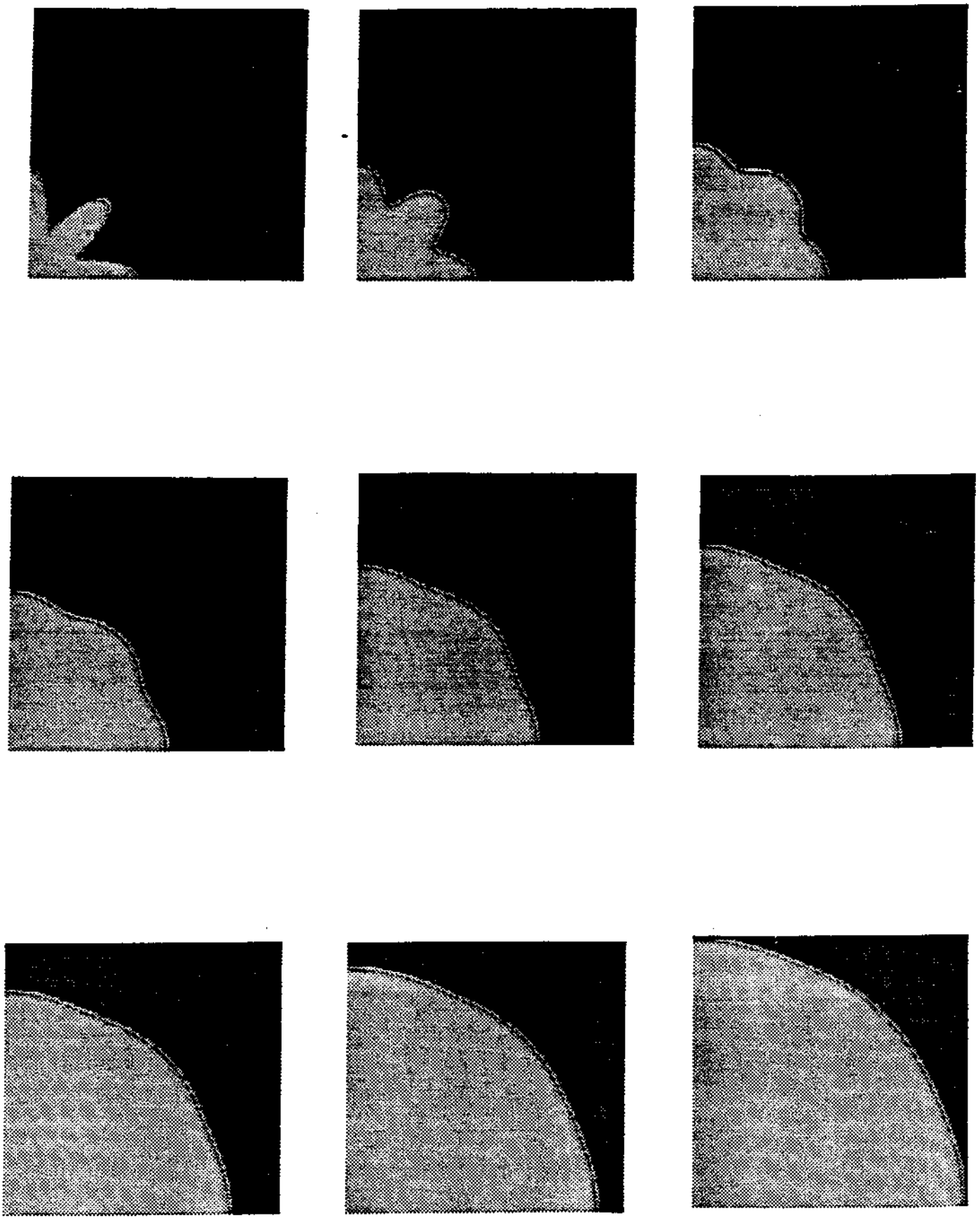

Fl(k 3,1

PVA Wulff Crystal

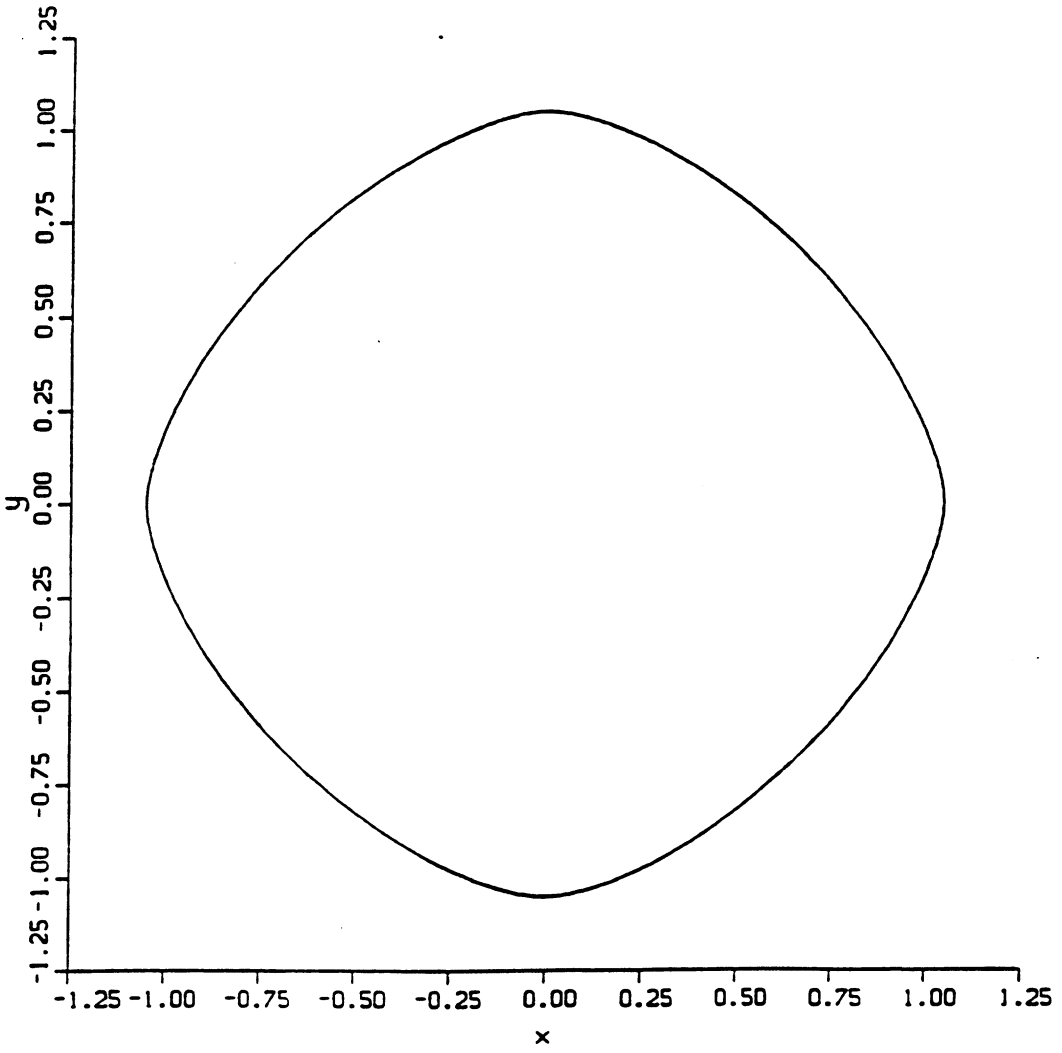

FIG. 3.2

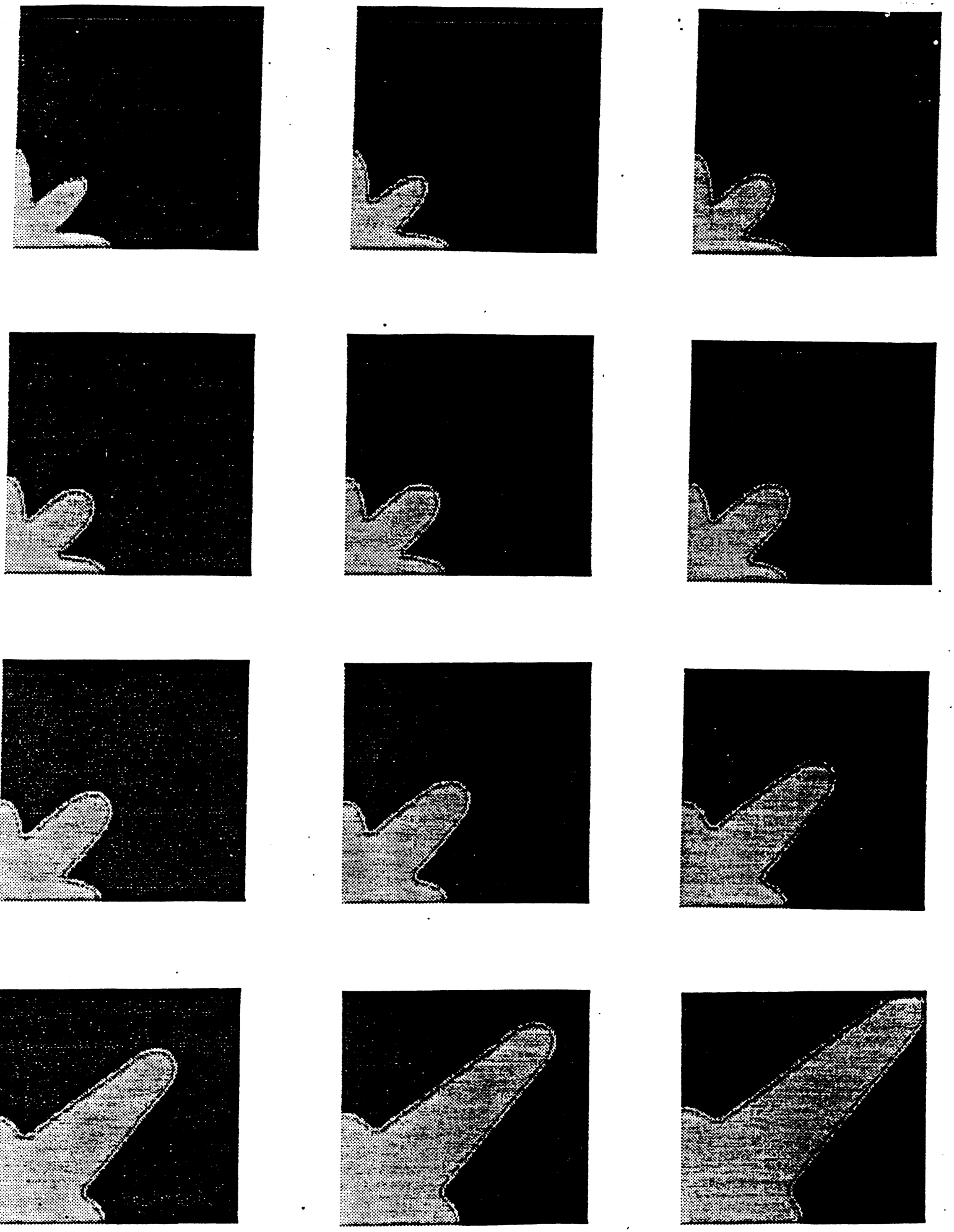

FIG. 4.1

TIP AND AXIS VELOCITIES OF NEEDLE CRYSTALS OBTAINED WITH DIFFERENT INITIAL INTERFACES

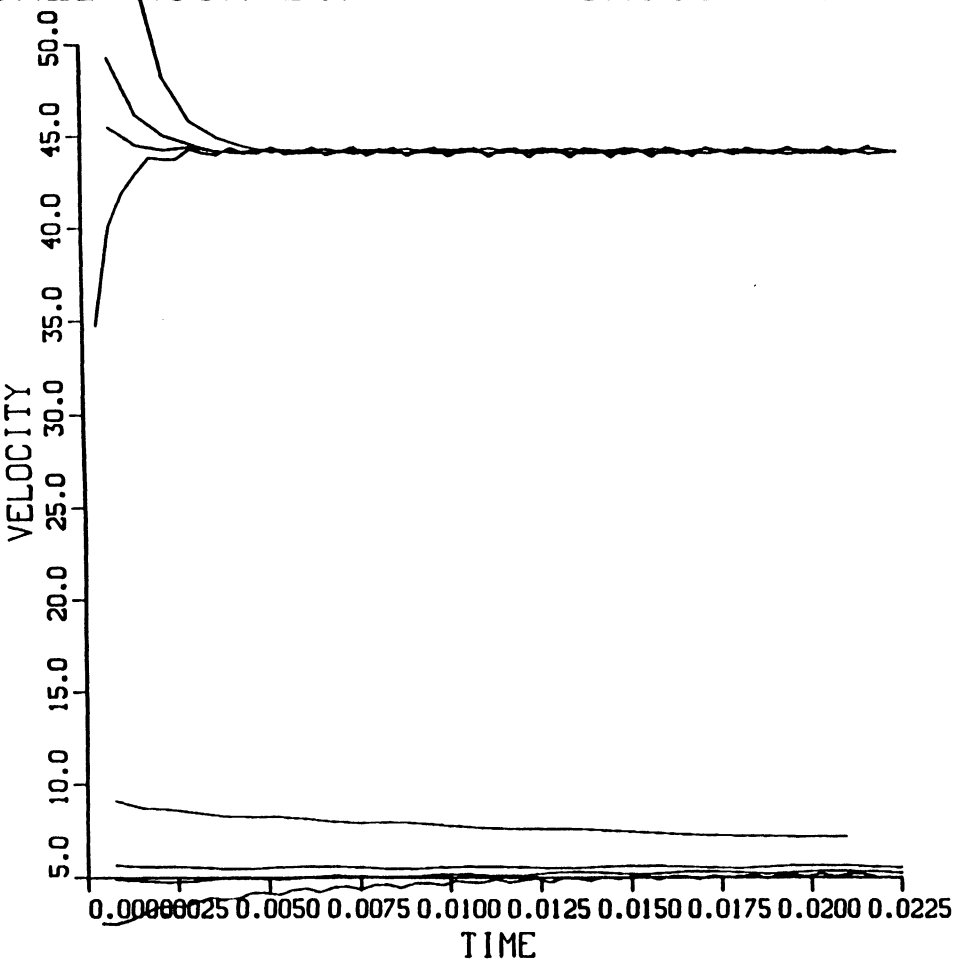

FIG. 4.2

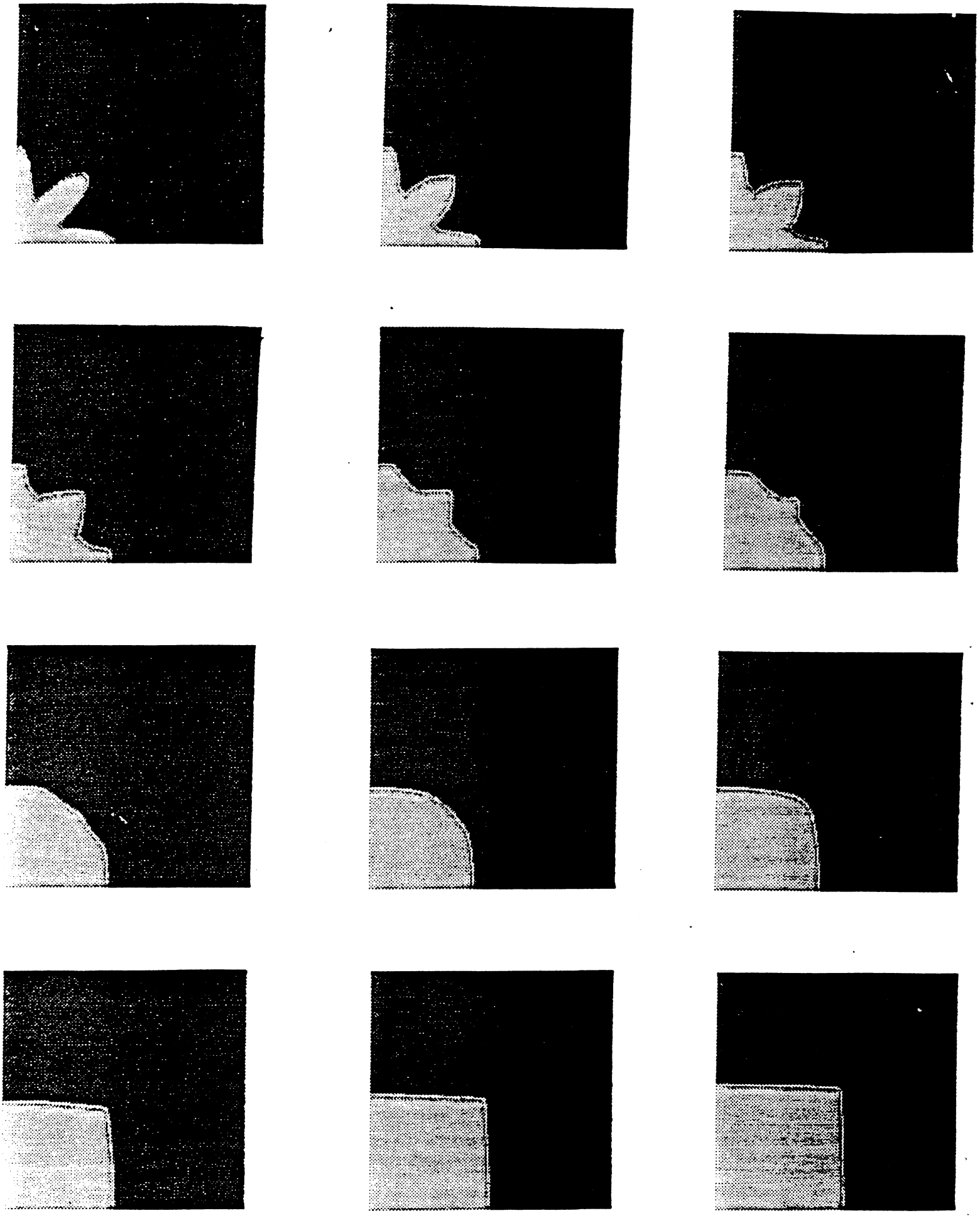

FIG. 5.1

MOTION BY MEAN CURVATURE
EXACT AND COMPUTED INTERFACE LOCATIONS
INITIAL INTERFACE IS A CIRCLE OF RADIUS 0.3

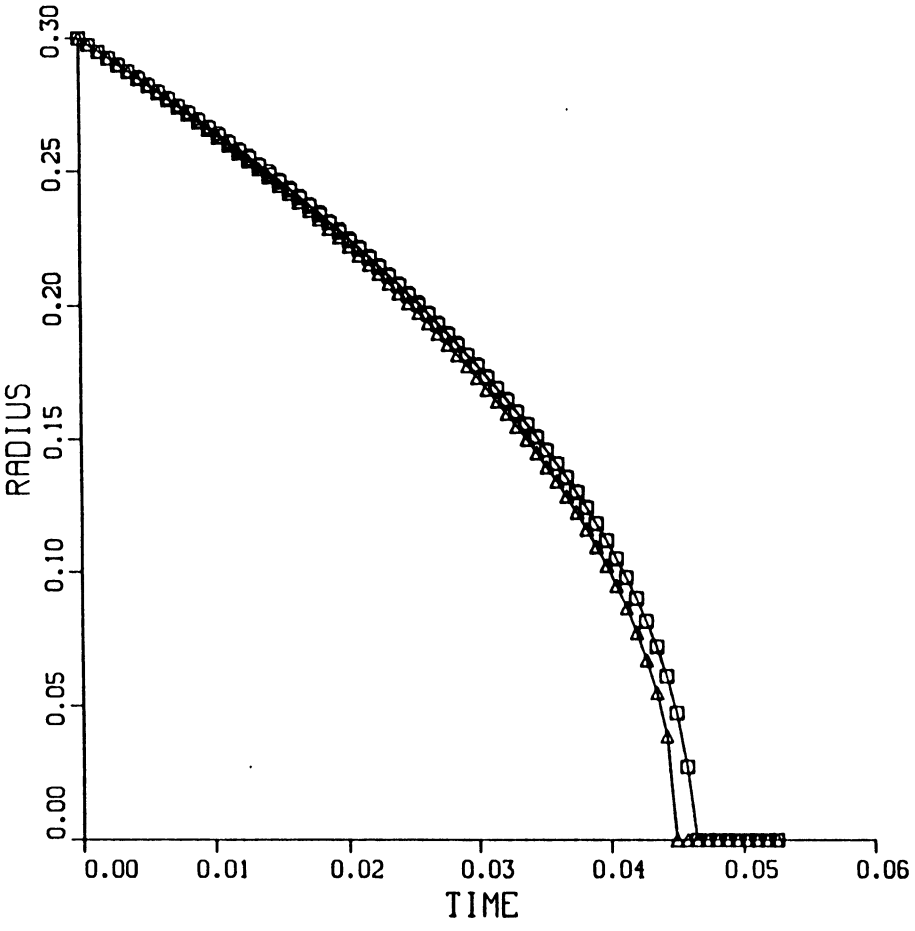

Fig. 6.1

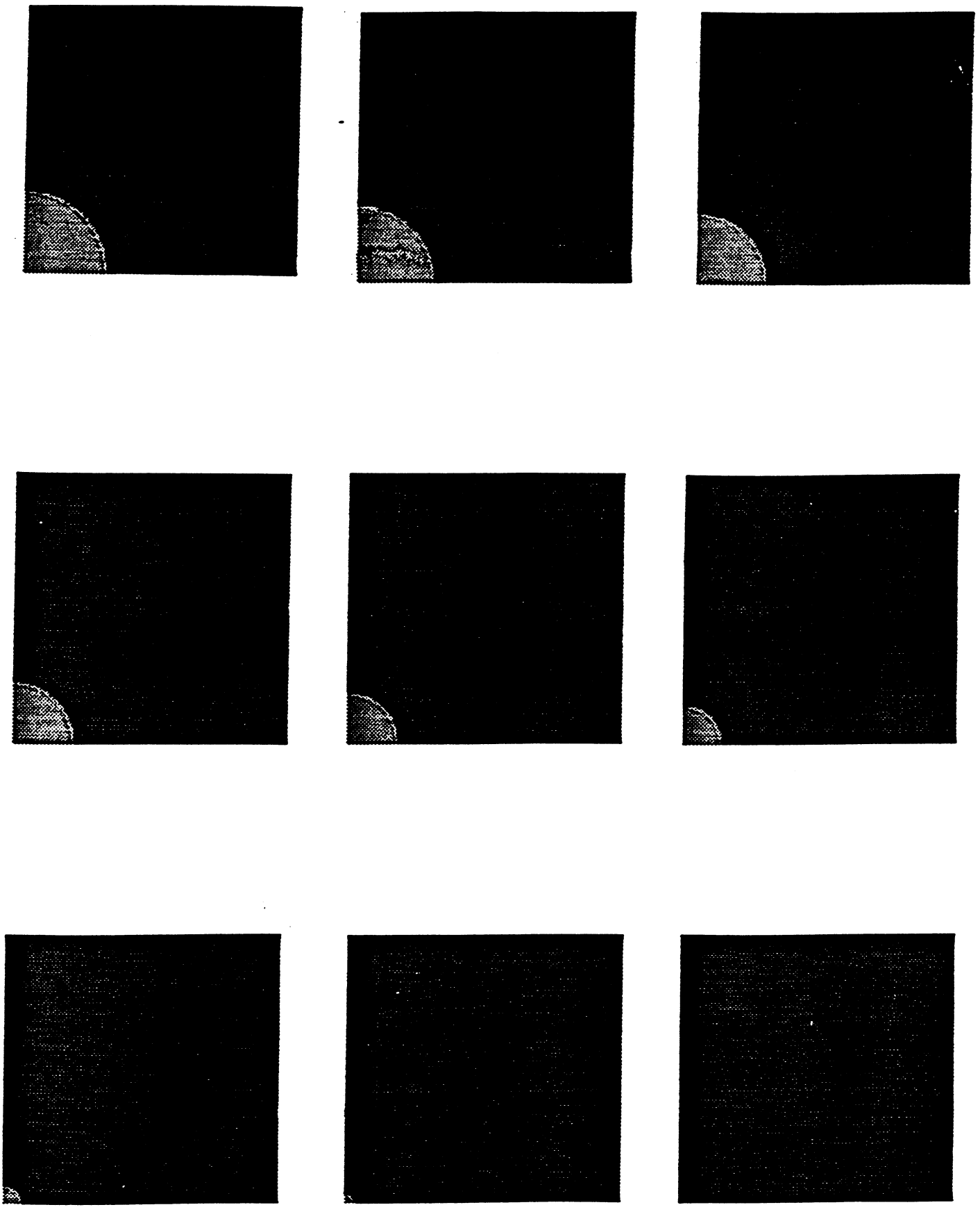

FIG. 6,2

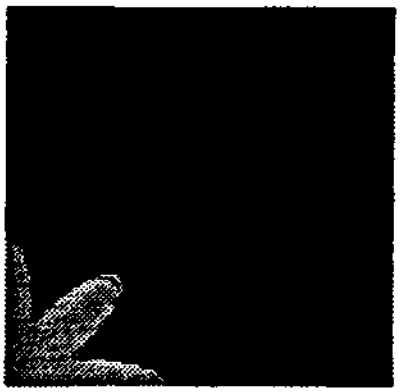
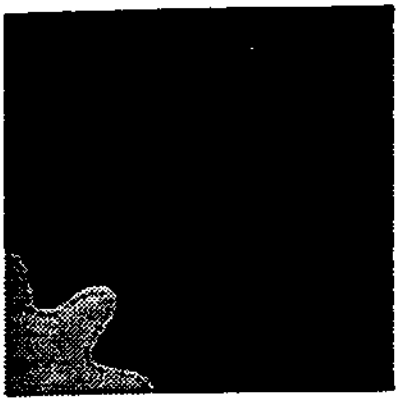
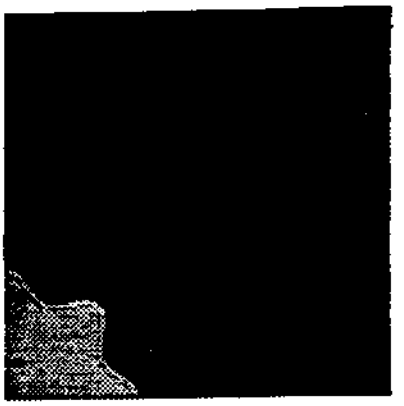
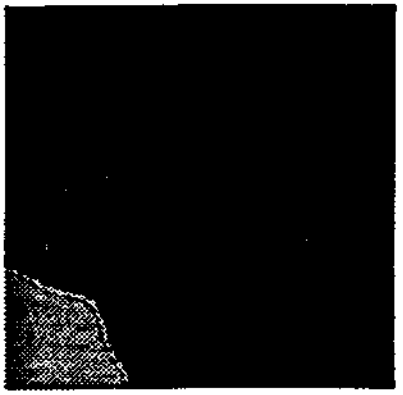
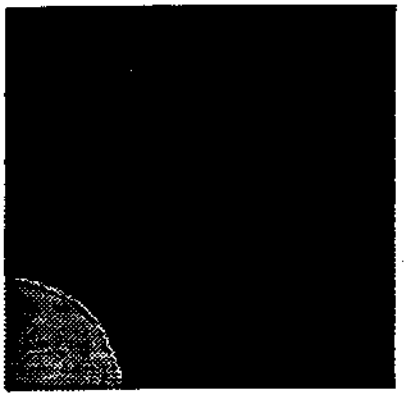
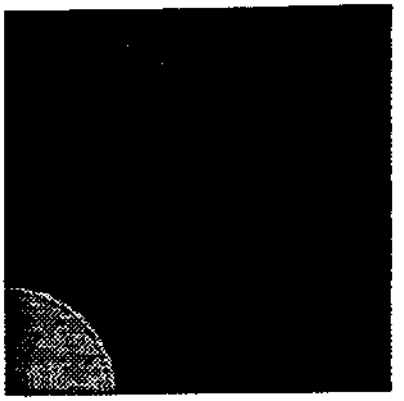
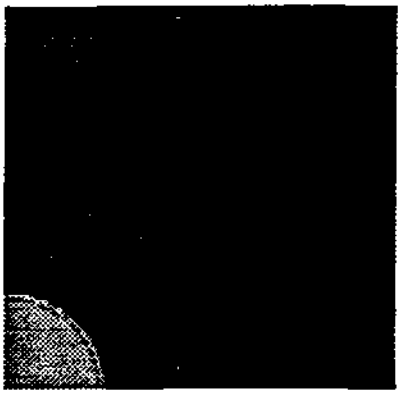
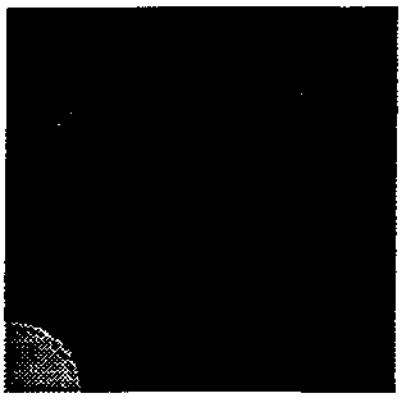


Rev031793

Center for Nonlinear Analysis
Report Series • Complete List

Nonlinear Analysis Series

No.

91-NA-001 [ ] Lions, P.L., **Jacobians and Hardy spaces**, June 1991

91-NA-002 [ ] Giga, Y. and Soto, M.-H., **Generalized interface evolution with the Neumann boundary condition**, July 1991

91-NA-003 [ ] Soner, H.M. and Souganidis, P.E., **Uniqueness and singularities of cylindrically symmetric surfaces moving by mean curvature**, July 1991

91-NA-004 [ ] Coleman, B.D., Marcus, M. and Mizel, V.J., **On the Thermodynamics of periodic phases**, August 1991

91-NA-005 [ ] Gurtin, M.E. and Podio-Guidugli, P., **On the formulation of mechanical balance laws for structured continua**, August 1991

91-NA-006 [ ] Gurtin, M.E. and Voorhees, P., **Two-phase continuum mechanics with mass transport and stress**, August 1991

91-NA-007 [ ] Fried, E., **Non-monotonic transformation kinetics and the morphological stability of phase boundaries in thermoelastic materials**, September 1991

91-NA-008 [ ] Gurtin, M.E., **Evolving phase boundaries in deformable continua**, September 1991

91-NA-009 [ ] Di Carlo, A., Gurtin, M.E., and Podio-Guidugli, P., **A regularized equation for anisotropic motion-by-curvature**, September 1991

91-NA-010 [ ] Kinderlehrer, D. and Ou, B., **Second variation of liquid crystal energy at x/|x|**, August 1991

91-NA-011 [ ] Baughman, L.A. and Walkington, N., **Co-volume methods for degenerate parabolic problems**, August 1991

91-NA-012 [ ] James, R.D. and Kinderlehrer, D., **Frustration and microstructure: An example in magnetostriction**, November 1991

91-NA-013 [ ] Angenent, S.B. and Gurtin, M.E., **Anisotropic motion of a phase interface**, November 1991

92-NA-001 [ ] Nicolaides, R.A. and Walkington, N.J., **Computation of microstructure utilizing Young measure representations,** January 1992

92-NA-002 [ ] Tartar, L., **On mathematical tools for studying partial differential equations of continuum physics: H-measures and Young measures**, January 1992

92-NA-003 [ ] Bronsard, L. and Hilhorst, D., **On the slow dynamics for the Cahn-Hilliard equation in one space dimension**, February 1992

92-NA-004 [ ] Gurtin, M.E., **Thermodynamics and the supercritical Stefan equations with nucleations**, March 1992

92-NA-005 [ ] Antonic, N., **Memory effects in homogenisation linear second order equation**, February 1992

92-NA-006 [ ] Gurtin, M.E. and Voorhees, P.W., **The continuum mechanics of coherent two-phase elastic solids with mass transport,** March 1992

92-NA-007 [ ] Kinderlehrer, D. and Pedregal, P., **Remarks about gradient Young measures generated by sequences in Sobolev spaces**, March 1992

92-NA-008 [ ] **Workshop on Shear Bands**, March 23-25, 1992 (Abstracts), March 1992

92-NA-009 [ ] Armstrong, R. W., **Microstructural/Dislocation Mechanics Aspects of Shear Banding in Polycrystals,** March 1992

92-NA-010 [ ] Soner, H. M. and Souganidis, P. E., **Singularities and Uniqueness of Cylindrically Symmetric Surfaces Moving by Mean Curvature**, April 1992

92-NA-011 [ ] Owen, David R., Schaeffer, Jack, andWang, Keming, **A Gronwall Inequality for Weakly Lipschitzian Mappings**, April 1992

92-NA-012 [ ] Alama, Stanley and Li, **Yan Yan, On "Multibump" Bound States for Certain Semilinear Elliptic Equations,** April 1992

92-NA-013 [ ] Olmstead, W. E., Nemat-Nasser, S., and Li, L., **Shear Bands as Discontinuities**, April 1992

92-NA-014 [ ] Antonic, N., **H-Measures Applied to Symmetric Systems**, April 1992

92-NA-015 [ ] Barroso, Ana Cristina and Fonseca, Irene, **Anisotropic Singular Perturbations - The Vectorial Case**, April 1992

92-NA-016 [ ] Pedregal, Pablo, **Jensen's Inequality in the Calculus of Variations,** May 1992

92-NA-017 [ ] Fonseca, Irene and Muller, Stefan, **Relaxation of Quasiconvex Functionals in BV(Ω,$\Re$P) for Integrands f(x,u,∇u)**, May 1992

92-NA-018 [ ] Alama, Stanley and Tarantello, Gabriella, **On Semilinear Elliptic Equations with Indefinite Nonlinearities**, May 1992

92-NA-019 [ ] Owen, David R., **Deformations and Stresses With and Without Microslip**, June 1992

92-NA-020 [ ] Barles, G., Soner, H. M., Souganidis, P. E., **Front Propagation and Phase Field Theory**, June 1992

92-NA-021 [ ] Bruno, Oscar P. and Reitich, Fernando, **Approximation of Analytic Functions: A Method of Enhanced Convergence**, July 1992

92-NA-022 [ ] Bronsard, Lia and Reitich, Fernando, **On Three-Phase Boundary Motion and the Singular Limit of a Vector-Valued Ginzburg-Landau Equation**, July 1992

92-NA-023 [ ] Cannarsa, Piermarco, Gozzi, Fausto and Soner, H.M., **A Dynamic Programming Approach to Nonlinear Boundary Control Problems of Parabolic Type**, July 1992

92-NA-024 [ ] Fried, Eliot and Gurtin, Morton, **Continuum Phase Transitions With An Order Parameter; Accretion and Heat Conduction**, August 1992

92-NA-025 [ ] Swart, Pieter J. and Homes, Philip J., **Energy Minimization and the Formation of Microstructure in Dynamic Anti-Plane Shear**, August 1992

92-NA-026 [ ] Ambrosio, I., Cannarsa, P. and Soner, H.M., **On the Propagation of Singularities of Semi-Convex Functions**, August 1992

92-NA-027 [ ] Nicolaides, R.A. and Walkington, Noel J., **Strong Convergence of Numerical Solutions to Degenerate Varational Problems**, August 1992

92-NA-028 [ ] Tarantello, Gabriella, **Multiplicity Results for an Inhomogenous Neumann Problem with Critical Exponent**, August 1992

92-NA-029 [ ] Noll, Walter, **The Geometry of Contact, Separation, and Reformation of Continous Bodies**, August 1992

92-NA-030 [ ] Brandon, Deborah and Rogers, Robert C., **Nonlocal Superconductivity**, July 1992

92-NA-031 [ ] Yang, Yisong, **An Equivalence Theorem for String Solutions of the Einstein-Matter-Gauge Equations**, September 1992

92-NA-032 [ ] Spruck, Joel and Yang,Yisong, **Cosmic String Solutions of the Einstein-Matter-Gauge Equations**, September 1992

92-NA-033 [ ] **Workshop on Computational Methods in Materials Science (Abstracts)**, September 16-18, 1992.

92-NA-034 [ ] Leo, Perry H. and Herng-Jeng Jou, **Shape evolution of an initially circular precipitate growing by diffusion in an applied stress field,** October 1992

92-NA-035 [ ] Gangbo, Wilfrid, **On the weak lower semicontinuity of energies with polyconvex integrands,** October 1992

92-NA-036 [ ] Katsoulakis, Markos, Kossioris, Georgios T. and Retich, Fernando, **Generalized motion by mean curvature with Neumann conditions and the Allen-Cahn model for phase transitions,** October 1992

92-NA-037 [ ] Kinderlehrer, David, **Some methods of analysis in the study of microstructure,** October 1992

92-NA-038 [ ] Yang, Yisong, **Self duality of the Gauge Field equations and the Cosmological Constant,** November 1992

92-NA-039 [ ] Brandon, Deborah and Rogers, Robert, **Constitutive Laws for Pseudo-Elastic Materials,** November 1992

92-NA-040 [ ] Leo, P. H., Shield, T. W., and Bruno, O. P., **Transient Heat Transfer Effects on the Pseudoelastic Behavior of Shape-Memory Wires,** November 1992

92-NA-041 [ ] Gurtin, Morton E., **The Dynamics of Solid-Solid Phase Transitions 1. Coherent Interfaces,** November 1992

92-NA-042 [ ] Gurtin, Morton E., Soner, H. M., and Souganidis, P. E., **Anisotropic Motion of an Interface Relaxed by the Formation of Infinitesimal Wrinkles,** December 1992

92-NA-043 [ ] Bruno, Oscar P., and Fernando Reitich, **Numerical Solution of Diffraction Problems: A Method of Variation of Boundaries II. Dielectric gratings, Padé Approximants and Singularities,** December 1992

93-NA-001 [ ] Mizel, Victor J., **On Distribution Functions of the Derivatives of Weakly Differentiable Mappings,** January 1993

93-NA-002 [ ] Kinderlehrer, David, Ou, Biao and Walkington, Noel, **The Elementary Defects of the Oseen-Frank Energy for a Liquid Crystal,** January 1993

93-NA-003 [ ] Bruno, Oscar P., Reitich, Fernando, **Numerical Solutions of Diffraction Problems: A Method of Variation of Boundaries III. Doubly Periodic Gratings,** January 1993

93-NA-004 [ ] James, Richard and Kinderlehrer, David, **Theory of Magnetostriction with Applications to** $Tb_xDy_{1-x}Fe_2$, February 1993

93-NA-005 [ ] Del Piero, Gianpietro and Owen, David R., **Structured Deformations of Continua,** February 1993

93-NA-006 [ ] Cheng, Chih-Wen and Mizel, Victor J., **On the Lavrentiev Phenomenon for Autonomous Second Order Integrands**, February 1993

93-NA-007 [ ] Ma, Ling, **Computation of Magnetostrictive Materials**, February 1993

93-NA-008 [ ] James, Richard and Kinderlehrer, David, **Mathematical Approaches to the Study of Smart Materials**, February 1993

93-NA-009 [ ] Kinderlehrer, David, Nicolaides, Roy, and Wang, Han, **Spurious Oscillations in Computing Microstructures,** February 1993

93-NA-010 [ ] Ma, Ling and Walkington, Noel, **On Algorithms for Non-Convex Optimization,** February 1993

93-NA-011 [ ] Fonseca, Irene, Kinderlehrer, David, and Pedregal, Pablo, **Relaxation in BV x L^∞ of Functionals Depending on Strain and Composition,** February 1993

93-NA-012 [ ] Izumiya, Shyuichi and Kossioris, Georgios T., **Semi-Local Classification of Geometric Singularities for Hamilton-Jacobi Equations**, March 1993

93-NA-013 [ ] Du, Qiang, **Finite Element Methods for the Time-Dependent Ginzburg-Landau Model of Superconductivity**, March 1993

93-NA-014 [ ] Chen, X., Hastings, S., McLeod, J. B., Yang, Y., **A Nonlinear Elliptic Equation Arising from Gauge Field Theory and Cosmology**, April 1993

93-NA-015 [ ] Gurtin, M., **Planar Motion of an Anisotropic Interface**, April 1993

Stochastic Analysis Series

91-SA-001 [ ] Soner, H.M., **Singular perturbations in manufacturing**, November 1991

91-SA-002 [ ] Bridge, D.S. and Shreve, S.E., **Multi-dimensional finite-fuel singular stochastic control**, November 1991

92-SA-001 [ ] Shreve, S. E. and Soner, H. M., **Optimal Investment and Consumption with Transaction Costs**, September 1992